A Network Analysis on Cloud Gaming: Stadia, GeForce Now and PSNow

designs

MDPI

Article

Design of an Optically Accessible Intake Manifold for Characterization of Liquid and Gaseous Jets in PFI Operating Conditions

Giovanni Cecere [1,2], Adrian Irimescu [1,*] and Simona Silvia Merola [1]

[1] CNR-STEMS Science and Technology Institute for Sustainable Energy and Mobility, 80125 Napoli, Italy
[2] Department of Energy (DENERG), Politecnico di Torino, 10129 Torino, Italy
* Correspondence: adrian.irimescu@stems.cnr.it

Abstract: The intake manifold and its components play a key role in the proper formation of air–fuel mixtures suitable for correct engine operation. In this article, starting from the original intake manifold design fitted to an optically accessible spark-ignited engine, a new solution was developed so as to allow the application of high-speed imaging of the fuel jet located between the runner and intake valves (Port Fuel Injection). To compare the two designs in terms of overall engine performance parameters such as volumetric efficiency, 0D/1D simulations were performed in motored conditions. Measurements at different crankshaft speed values were used for calibrating the intake line parameters and providing boundary conditions. Finite Element Analysis (FEM) was performed in SolidWorks to verify the structural strength of the new design when operating in the most critical conditions, i.e., boosted operation. As an overall conclusion, the results show that the new design guarantees a wider range of intake pressure values during the intake stroke, thus expanding the possible operative points. This can be obtained without compromising structural integrity, given that predicted safety factors were well above acceptable limits even for relatively high boost levels.

Keywords: improved multi-objective design; intake manifold; spark ignition engine; optical accessibility

Citation: Cecere, G.; Irimescu, A.; Merola, S.S. Design of an Optically Accessible Intake Manifold for Characterization of Liquid and Gaseous Jets in PFI Operating Conditions. *Designs* **2023**, *7*, 24. https://doi.org/10.3390/designs7010024

Academic Editor: Wenbin Yu

Received: 19 December 2022
Revised: 9 January 2023
Accepted: 10 January 2023
Published: 1 February 2023

1. Introduction

In the scenario of growing demand for increased engine efficiency towards the adoption of further stringent norms given by the European Euro VII regulation [1], the search for new loopholes wherever there is any scope for improvement became one of the main challenges for the researchers in this field. The design phase of internal combustion engines (ICEs) is centered on the main process, i.e., combustion itself, as well as all the consequent factors of influence that range from the intake conditions to exhaust emissions. This applies to both main categories, i.e., spark ignition (SI) [2] and compression ignition (CI) units [3,4], even if significant differences can be evident at the component level. In this multi-objective problem, great effort is employed to design the intake manifold. This component has evolved over the years, both in terms of performance [5–7] and materials [8]; proper design ensures a reduction of the overall environmental impact (with direct effects on emissions) and a more sustainable life cycle assessment (LCA). Given its key role in the overall system configuration, ever more complex shapes and variable geometries have been developed with the support of computational fluid dynamics (3D CFD) codes so as to comply with a multitude of requirements. One of the most investigated aspects is the optimization of volumetric efficiency over a wide range of engine speed and load conditions, with increased complexity, especially for multi-cylinder engines. Silva et al. in [9] carried out an analysis of the intake runner length and how it influenced the performance of a four-cylinder SI engine. The conclusions of this work, given by the experimental tests coupled with the use of 0D/1D numerical simulations, showed different optimum runner lengths for each

engine speed considered, then suggesting the use of a variable geometry technology for vehicles subject to different drive cycles (e.g., urban mobility vehicles). In [10], the authors performed a similar investigation, where the possibility to directly vary the main plenum volume of the intake manifold was scrutinized; it demonstrated how with this type of solution, it was possible to gain higher volumetric efficiency and lower fuel consumption for the engine speeds for which the original design was not optimized. Variable runner length was examined by Otávio et al. in [11], where the authors performed numerical simulations to find that it was possible to achieve the best volumetric efficiency condition for a certain speed; thus, the authors noted the achievement of higher engine performance for each operative condition examined. Other applications related to intake manifold design include the improvement of driving experience, for instance, by reducing the turbo-lag phenomenon [12] or employing specific devices to increase the inlet flow density [13] for racing applications. In addition, within the context of using alternative energy carriers and hybrid powertrain solutions [14], the intake manifold design, coupled with that of the intake valves, can play a relevant role in the probability of backfire phenomena when using hydrogen [15]. Furthermore, in the context of reducing emissions, several studies have proved the benefits of optimizing overall geometry characteristics [16,17]. For diesel power units, improved design of the intake manifold can ensure the abatement of soot emissions [18] that can be further reduced by using alternative fuels [19,20].

A detailed understanding of underlying phenomena can bring additional margins for improvement, and the use of optically accessible engines [21] provides unique opportunities for applying high spatial resolution techniques [22]. These can ensure valuable insight into particular operating characteristics such as cycle-to-cycle variability [23,24], flame kernel inception, and in-cylinder formation of pollutants [25]. Specific investigations aimed at phenomena that take place in the intake manifold range from "simulated" rigs for studying fuel jets and related interactions [26] to local access for an optical fiber for determining liquid film parameters [27] or custom setups for investigating backfire in H_2 engines [28]. The use of 3D CFD simulation is becoming ever more spread for research and development [29], and the optical techniques ensure valuable data for model validation. This provides the basis for solving particular issues that can hinder the application of alternative fuels, such as hydrogen [15,30], that features significant potential for achieving carbon-free energy and transportation.

This work developed a new intake manifold designed for optical accessibility while ensuring the complete functionality of the single-cylinder engine it would be fitted to. More to the point, the engine features a cylinder head taken from a commercial four-cylinder unit that was adapted for the bottom part that is adapted with an elongated piston for optical accessibility. Therefore, the new component would have to ensure improved functionality compared with the outgoing part intended for four cylinders and, at the same time, allow the application of optical techniques. Two windows on the plenum were therefore included during the initial sketch phase so as to comply with the latter requirements. Given that the base configuration of the engine features gasoline direct injection (GDI) operation, an injector was positioned close to the intake valves for the new component, thus ensuring PFI operation as well. As a first step of design validation, a finite element analysis was performed to verify safety factor ratings in static conditions. The new component was compared with the existing situation in terms of functionality by applying 0D/1D simulation. Experimental data recorded at 1000 and 2000 rpm in motored conditions was used for model calibration and validation.

2. Engine Setup

Figure 1 illustrates the overall layout of the engine taken as the starting point for this study; its main components are highlighted as well. Specifications are listed in Table 1. Overall, the idea was to use an original equipment manufacturer (OEM) cylinder head (taken from a turbocharged GDI inline-four SI engine) and adapt it to be fitted to the research engine block. An adapter flange was therefore designed and fitted between the

head and block. The bottom part features an elongated Bowditch piston [31]; this design allows a 45 deg inclined mirror to be fitted and thus ensures the bottom view into the combustion chamber via a quartz window in the piston crown. The compression ratio (CR) can be varied by modifying the number of spacers between the head and single-cylinder engine block; for the current work, a nominal value of 10 was set. All the data used for calibrating the 0D/1D model were acquired in motored condition for two engine speed values, 1000 and 2000 rpm, and different throttle valve openings. The choice of using motored data only was made for minimizing the influence of combustion on fluid dynamics (even if overall the effects on the intake process are reduced); the rpm range was limited by the additional mass of the elongated piston, but for the scope of the present work the data can be considered as representative enough. For each condition, 200 consecutive cycles were recorded with a resolution of 0.2 CAD per cycle and an accuracy of ±0.5% given by the piezo-electric pressure transducer flush mounted with the cylinder head surface.

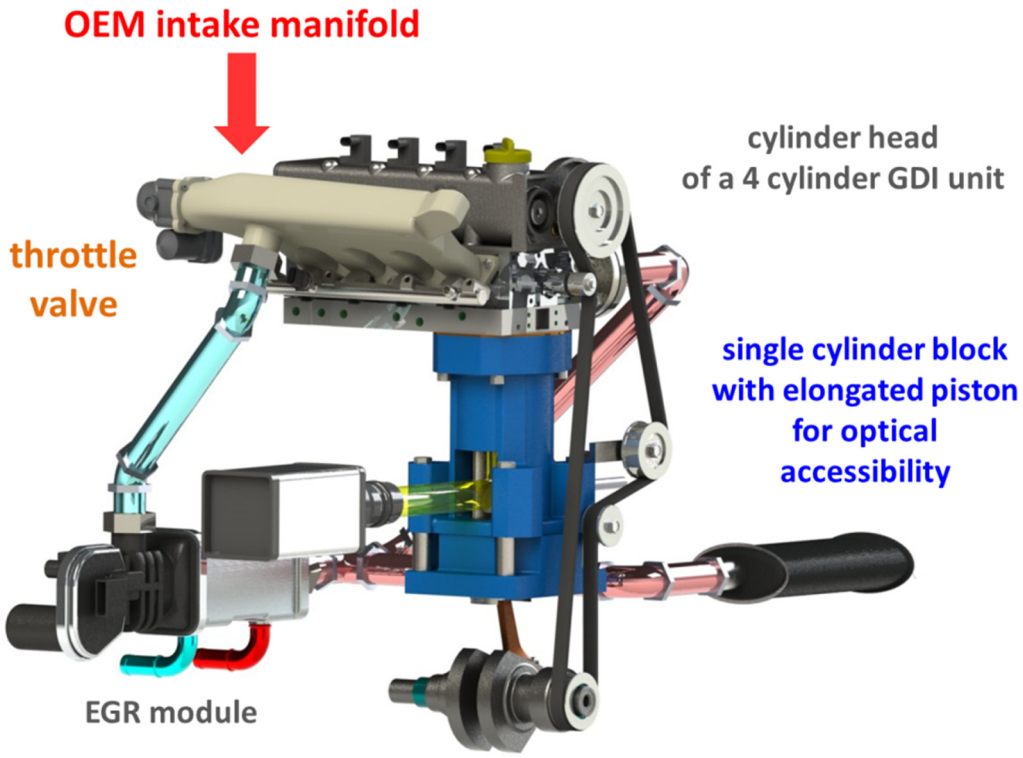

Figure 1. Illustration of the engine used for the experimental trials; the crankshaft housing is not shown so as to render the length of the elongated piston part.

Table 1. Engine specifications.

Engine Specification	
Number of cylinders	1
Compression ratio	10:1
Bore	79 mm
Stroke	81.3 mm
Number of valves	4
Injection setup	direct injection wall guided
Exhaust Valves Open	153 CAD aTDC
Exhaust Valves Close	360 CAD aTDC
Intake Valves Open	363 CAD bTDC
Intake Valves Close	144 CAD bTDC

3. 3D Model

As previously iterated, the main goal was to ensure optical accessibility close to the point of injection (i.e., at the end of the intake runners and close to the valves). Two windows would have to be placed on the manifold walls so as to ensure a wide range of optical techniques are applied. The complex geometry of the OEM part and the fact that it is built in plastic did not allow extensive modifications. Therefore, a new component was designed so as to achieve the main goal. Apart from the possibility of inserting an endoscope for visualizing fuel jets in the intake port, the location available on the manifold wall would also allow an additional injector to be fitted and, thus, multiple configurations to be compared (e.g., combined liquid and gas injection). Figure 2 illustrates the difference between the old (Figure 2a,b) and new (Figure 2c,d) parts, as well as possible configurations for applying high-speed visualization. It is immediately evident that the OEM manifold does not feature a seating location for the PFI injector; therefore, the design includes this option, with the seat inclined at an angle that allows correct spray targeting with respect to the intake valves. The choice of material was made so as to make use as much as possible of semi-finished products, ensure the required strength and render possible certain operating conditions that may require increased air temperature (e.g., HCCI); therefore, steel was chosen. The actual shape of the new part is the result of several single components welded together. For example, the intake manifold was assumed to be a rectangular tube $60 \times 40 \times 2$ mm, a standard semi-finished material; it would have to be 90 mm long, feature two rectangular cuts on the 40 mm high walls, and three holes on the 60 mm wide side. The runner instead is a $50 \times 25 \times 2$ mm rectangular tube, with a cut inclined at 65 deg with respect to the 50 mm wide base, and worked with a 20 mm drill fitting the injector seat. These two components welded together constitute the core of the intake manifold, on which the other parts would be welded (e.g., the flange for coupling with the cylinder head or that for fitting the throttle valve). The approach allows a complex assembly to be obtained without the need for molding.

Given that the upper part of the engine was adapted from the commercial unit, the intake manifold featured four runners and a large plenum (i.e., the commercial power unit featured 1.4 L displacement, roughly 3.5 times that of the single-cylinder research engine). This ensures good volumetric efficiency at wide open throttle (WOT) but reduces the range in which load can be varied. More to the point, the throttle valve has a non-zero discharge coefficient even when it is completely closed (to ensure a minimum flow of air in case of failure of its electric actuation), and thus the intake pressure cannot be reduced below a certain threshold for the single cylinder application. This greatly diminishes the load range for the intended use, e.g., with the throttle completely closed, intake pressure at the bottom dead center (BDC) was close to 0.8 bar at 1000 rpm, while during normal operation, this would be as low as 0.2–0.3 bar for a multi-cylinder engine. Hence the volume of the new part would have to be greatly reduced compared with the outgoing one. As a rule of thumb, one-fourth of the OEM manifold volume was taken as the starting point. Additional requirements of placing various sensors and simplified geometry constraints resulted in a final value of just under a third of the overall volume of the old component.

Figure 2 illustrates several other access points in addition to the two windows intended for optical investigations. One is for the intake manifold pressure sensor (the raised flat surface with two holes, one for access to the measurement volume and the other for fixing the sensor); it practically emulates the fitting position of the elongated appendix shown on the top-left side of Figure 1 (on the opposite end of the manifold with respect to the throttle valve). The other two access points feature G1/4" coupling and allow other sensors to be connected (e.g., a thermocouple) or the exhaust gas recirculation (EGR) line.

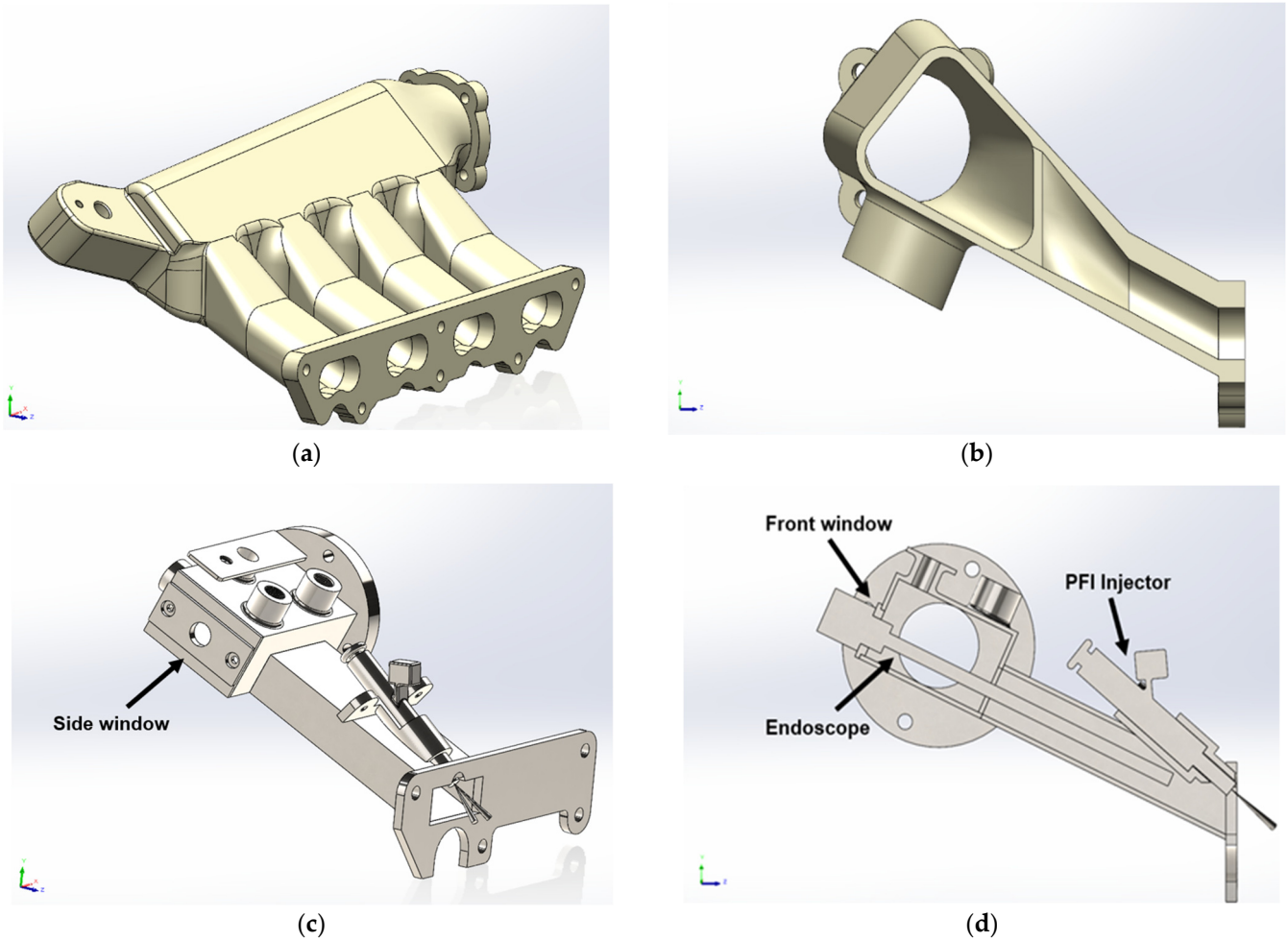

Figure 2. 3D model of the original intake manifold (**a**) and cross-section (**b**). 3D model of the new design (**c**) and related cross-section point of view (**d**).

Once the new design was completed, a finite element analysis (FEM) was performed on the part so as to verify the capacity to guarantee reliable safety factors for all the conditions in which it is intended to operate. The sub-components were considered welded together, and the outer pressure was taken as 1 atm. The inner pressure was imposed as a distributed force acting perpendicularly to the surfaces from the inside to the outside, equal to the absolute inlet pressure. The load relative to the weight of the components was discharged on the mounting screws and in the resulting center of gravity of the assembled body. In order to improve the FEM analysis, the highest definition of the mesh available was chosen, corresponding to elements with a variable length between 0.2 and 4.0 mm, depending on the local geometry. Figure 3 shows the results obtained from the static analysis at the maximum level of boosting considered, i.e., an absolute intake pressure of 2.5 bar. The maximum stress highlighted in the figure was detected on the lower side, between the runner and the connection plate; there is very good margin with respect to the Von Mises yield value (Figure 3a, a scale of 100:1 was used to highlight the deformation). The lowest safety factor (indicated as FOS in Figure 3b) value is around 2.8, recorded in the same area (Figure 3b). It should be noted that the presence of weld beads was not taken into account for the analysis, and it is reasonable to assume that the true safety factor is even higher. After implementing the static approach, the dynamic behavior was analyzed by employing the function built into Solidworks that is able to give a first evaluation of the dynamic behavior of the treated component; no critical failure phenomena related to fatigue stress were predicted. Further dynamic analysis was carried out by imposing one hundred million cycles characterized by the variable load in terms of pressure variations

from atmospheric (e.g., WOT operation) to the maximum boost condition (i.e., 2.5 bar absolute). No significant influence of the load linked to the weight of each component was noted. The results of the more detailed dynamic analysis confirmed the overall conclusion of the first evaluation, meaning that there were no significant effects on the integrity of the part, and the entire intake manifold did not present any relevant aging phenomenon due to fatigue stress.

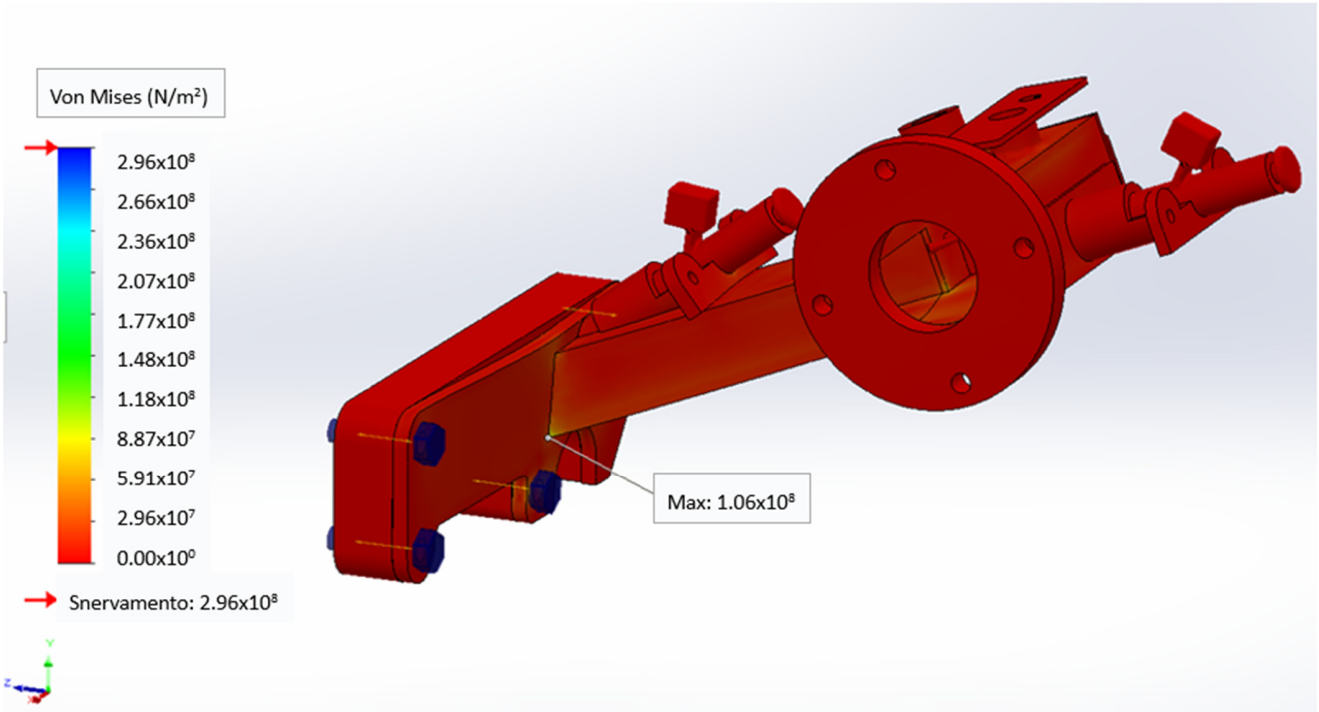

(**a**)

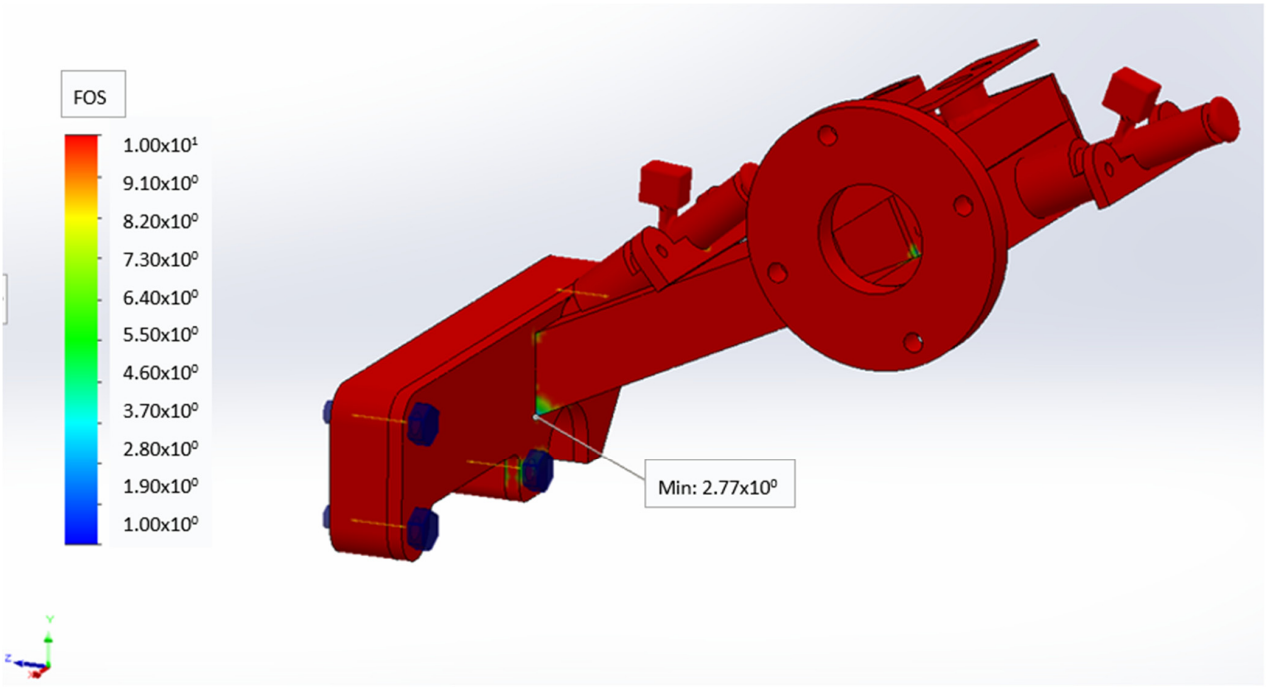

(**b**)

Figure 3. FEM static approach: stress analysis result (**a**) and safety factor (FOS) evaluation (**b**); two injectors are also shown fitted in the port- and manifold wall.

One interesting assessment would be to investigate the negative effects of unwanted phenomena such as backfire (not uncommon for port-fuel injection H_2 engines). The sudden increase in local pressure could determine a more pronounced influence of fatigue. A possible route for further analyzing such conditions would be to simulate a pressure profile inside the intake manifold with 0D/1D or 3D CFD codes and then impose such a variation in Solidworks. This could also be coupled with the results of optical investigations that would provide more detailed confirmation of fuel distribution during the injection.

4. Numerical Model

Once it was clarified that the new component was sound in terms of structural integrity, its actual applicability was investigated with respect to the achievable intake pressure range. This was implemented in a 0D/1D simulation framework that can predict overall parameters such as absolute pressure, volumetric efficiency, or fluid composition [24,32]. A model was built in the GT-Suite software [33], with two versions of the intake manifold. Figure 4a highlights the two equivalent components that model the manifold. Basically, for the old version, it is a series of T elements (the plenum) connected to round pipes (the runners), with one of these endings with a Y shape splitter that goes to the two intake ports, one for each valve. Evidently, the only difference between the two models is the number of runners (reduced from four to one for the new component).

The basic approach of the 1D simulation code is to apply conservation equations of mass, energy, and momentum in several sub-domains of the model; their discretization length is imposed by the user (the computational effort depends on this parameter, intuitively, the shorter the discretization length, the longer it takes to complete the simulation of one cycle). In the volumes used for modeling the overall components, the scalar quantities, such as pressure, temperature, density, internal energy, and so on, are considered to be homogeneous, while the vector variables (i.e., mass flow rate, velocity, etc.) are calculated along the boundaries. Figure 4b shows a simplified illustration of the 1D approach.

Data recorded with the old manifold design were used for model validation. Simulated and measured traces were compared for the intake plenum and cylinder. It should be noted that absolute pressure in the T element was monitored at the location of the pressure sensor placed at the end of the manifold, as shown in Figure 1. Forward and backward discharge coefficients of the throttle valve were imposed in the model based on OEM data. More to the point, the old manifold features a 44 mm diameter valve, for which a flow of 878 kg/h is specified at a pressure drop of 600 mbar and 297 K air temperature when the throttle angle is 85 deg [34]. A simplified model was built to simulate the throttle valve only, and the flow results were within 1% of the OEM data.

Figure 5 illustrates the comparison between the experimental and simulated pressure traces at 2000 rpm, with a fully closed throttle valve and WOT conditions during motored operation. A good agreement can be observed for the low (Figure 5b) as well as high-pressure (Figure 5a) parts of the working cycle. More consistent differences were recorded for the 0% opening case in terms of intake manifold pressure. Nonetheless, the fact that in-cylinder pressure was correctly modeled for both situations gives confidence in the results that were obtained when assessing the new manifold configuration.

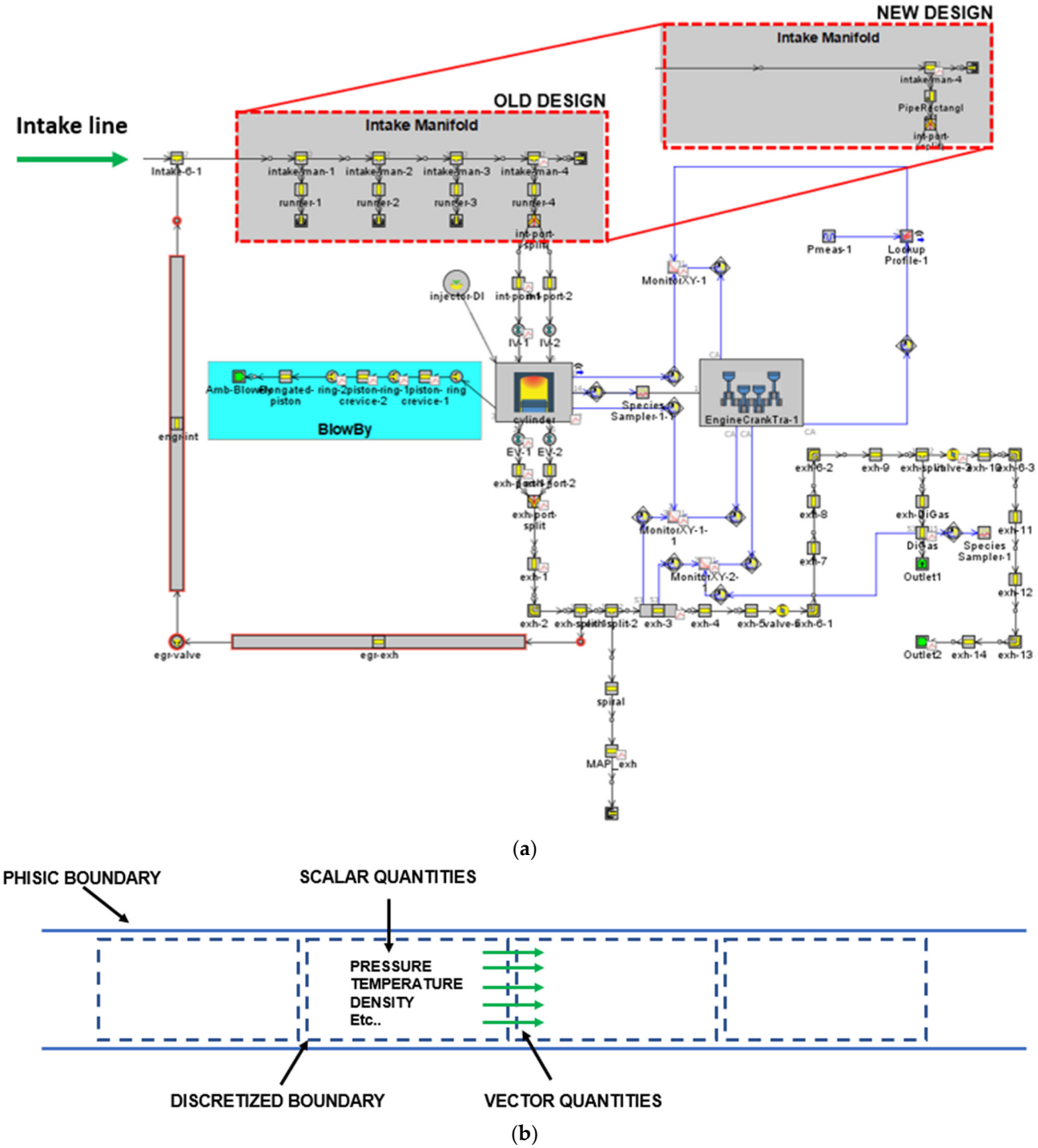

Figure 4. Layout of the engine simulation model (**a**) and schematic illustration of a discretized grid (**b**) for the one-dimensional approach.

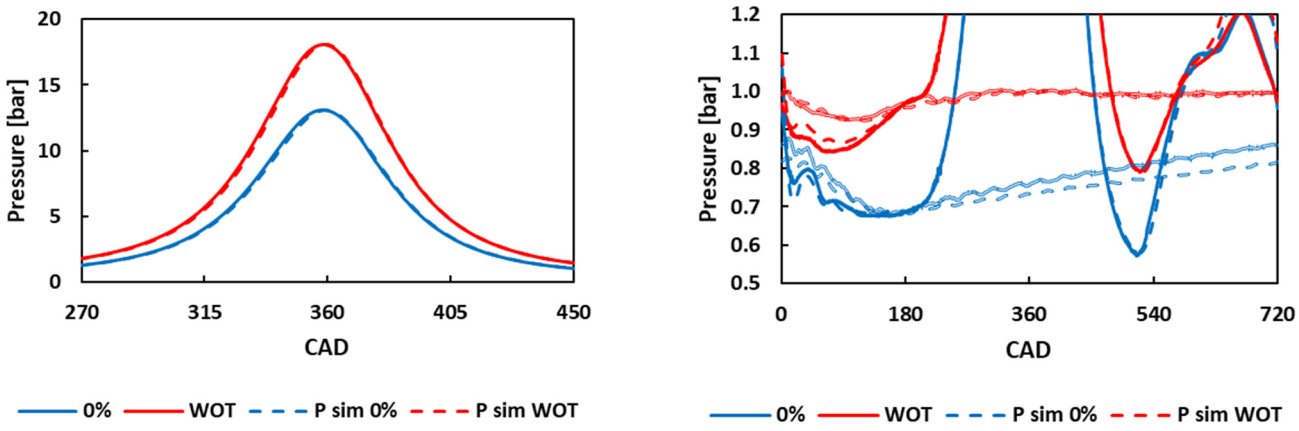

Figure 5. Simulated (dashed lines) and measured (solid lines) in-cylinder pressure traces at 2000 rpm, WOT, and completely closed throttle (**a**); the low pressure range also shows intake pressure traces (**b**).

5. Results

Several engine tests have been performed at different crankshaft velocities and throttle valve openings. Table 2 lists the conditions during which intake and in-cylinder pressure were measured. The same points were also simulated using the 0D/1D model. One important parameter that needed to be implemented was the discharge coefficient (C_d) of the throttle valve. No actual airflow measurements were available (they would be difficult to implement due to the single-cylinder architecture and resulting highly pulsating flow), and therefore, an alternative was needed for determining the C_d profile at various throttle opening percentages. The 0D/1D model was used for simulating in-cylinder pressure traces, and these were compared with the measurements. More to the point, each operating condition featured an imposed C_d value that was adjusted to match the measured in-cylinder pressure. The resulting profile was then used for performing the simulation with the new component.

Table 2. Operative conditions.

Engine Condition	Speed [rpm]	Throttle Valve Opening [%]
Motored	1000	0-5-10-15-100
	2000	0-1-2-3-4-5-10-15-20-50-100

Figure 6a,b show the volumetric efficiency obtained by performing simulations with the old and new design; measured peak in-cylinder pressure (Figure 6e,f) and at intake BDC (Figure 6c,d) are also shown with square symbols (for the old manifold design). Overall the agreement between numerical and experimental results can be judged as good throughout the range of conditions that were investigated. This further highlights that the calculated volumetric efficiency are valid results that can be used for evaluating the new component.

As expected, the smaller volume manifold ensures a wider range of flow (and, indirectly, more extensive variations of volumetric efficiency). One essential result is that at WOT, there was an insignificant effect of the new design (i.e., around a 1% gain in volumetric efficiency was predicted compared with the outgoing component). This is mainly due to the fact that the actual length of the runners was kept practically the same (thus maintaining a similar response with respect to pressure fluctuations [7]), and a comparable cross-section was ensured in the manifold; therefore, the full load flow characteristics were maintained, while allowing more throttling to be applied.

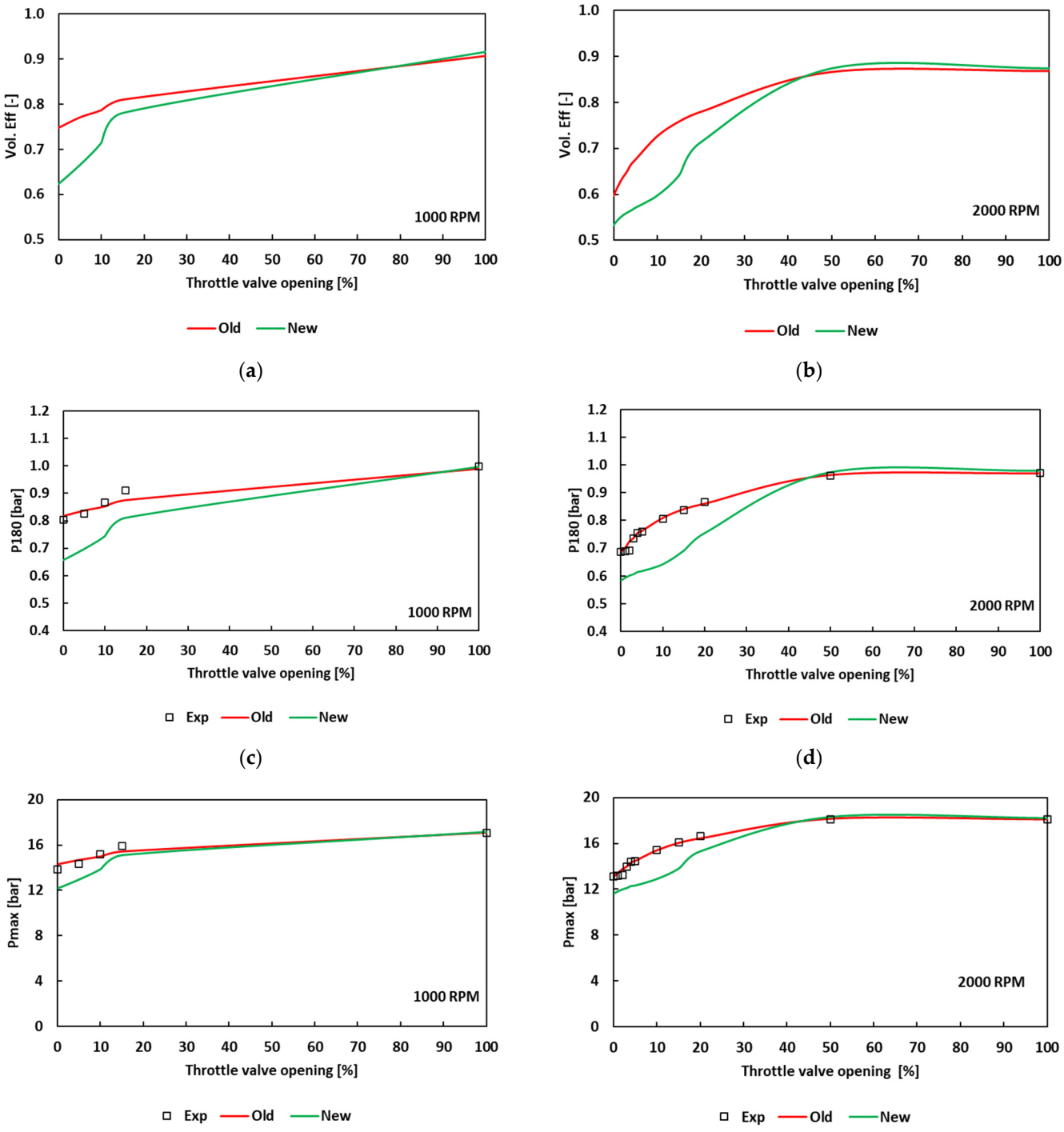

Figure 6. Volumetric efficiency, in–cylinder pressure at 180 deg bTDC, and its peak value for motored conditions at 1000 (**a**,**c**,**e**) and 2000 rpm (**b**,**d**,**f**); measurements are sown (only for the old design) with squared symbols.

The overall conclusion is that at 1000 rpm, the new design ensures a volumetric efficiency interval close to 30%, compared with only around 15% for the four runners part. The increase in range was less evident at 2000 rpm, but nonetheless, there was an improvement. With respect to the correlation between the actuated parameter (throttle angle) and flow dependency, roughly the same behavior can be observed, meaning that at

1000 rpm significant reduction of the volumetric efficiency is obtained below 20% throttle opening, while at 2000 rpm, the threshold was around 45%.

As a direct consequence of the reduced plenum and runner volume for the new part, the predicted peak pressure was considerably lower when the throttle valve was completely closed (Figure 7a,b). The graphs also illustrate more extensive throttling during the intake stroke at 0 valve opening, while at WOT, the pressure traces were practically the same. This further emphasizes the fact that functionality was significantly improved while maintaining full-load performance. These positive results come without major loss in volumetric efficiency at high load; as previously iterated, at WOT, an insignificant variation was recorded between the old and new designs. Even more, simulations performed in supercharged conditions predicted only 1% lower volumetric efficiency with a boost pressure of 1.5 bar; more to the point, to obtain the same airflow, only 15 mbar of boost needs to be applied compared with the old manifold design.

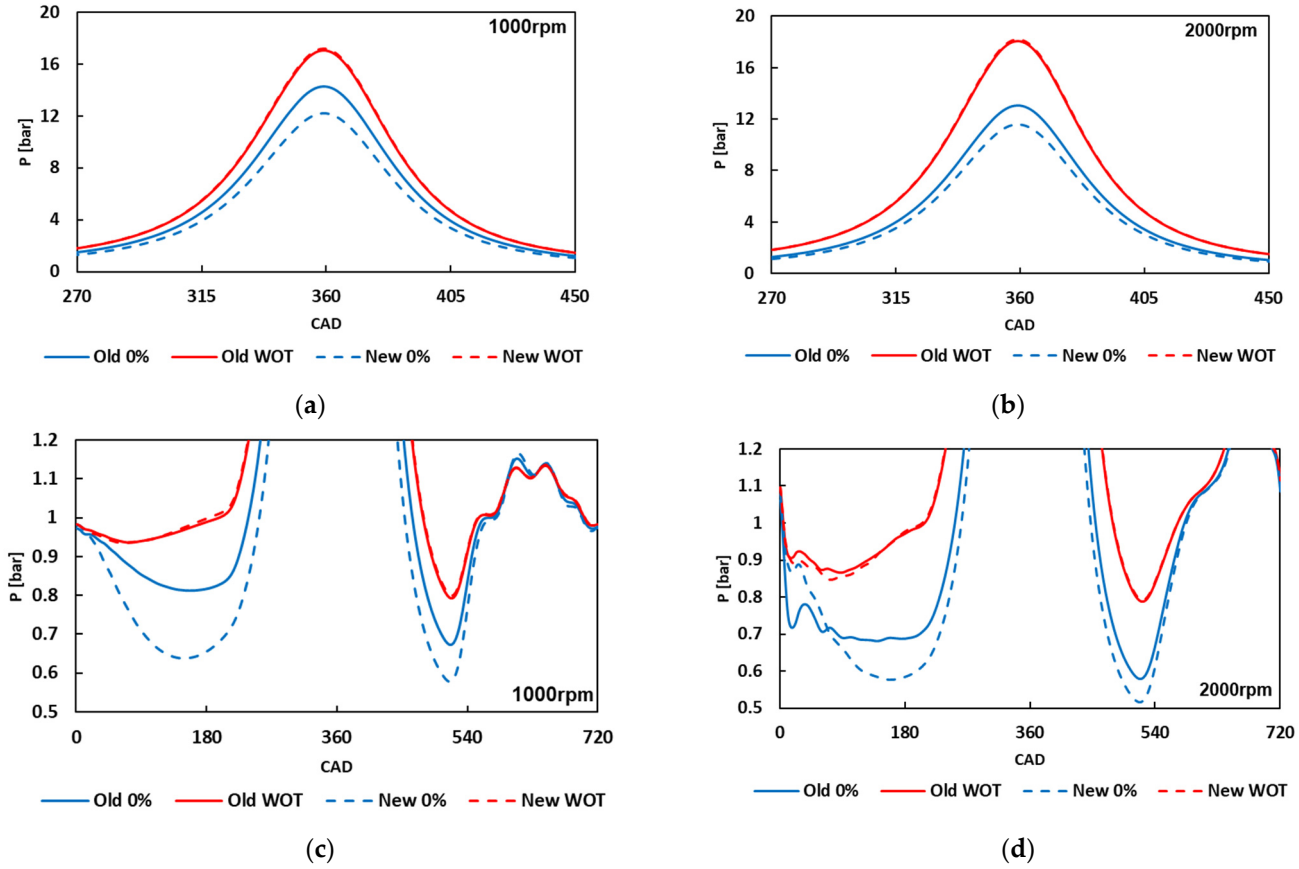

Figure 7. In-cylinder pressure traces at 1000 (**a**,**c**) and 2000 rpm (**b**,**d**) for the old (solid lines) and new (dashed lines) intake manifold design.

Another aspect that needs to be considered is that the design point for the throttle valve itself was correlated to the four-cylinder engine. Therefore, it is very likely that choosing a throttle with a smaller diameter (e.g., 32 mm compared with the existing 44 mm) would further enhance the range of achievable intake pressure. Unfortunately, there was no data available for building a detailed discharge coefficient profile for such a situation. Tests and simulations that include this parameter as well are an interesting line of development of the current research. 3D CFD simulations would also provide means for gaining valuable insight into the flow characteristics around the components that will be inserted during the optical investigations (e.g., the endoscope) and how these may influence fuel jets and resulting air-fuel mixture formation.

6. Conclusions

A novel intake manifold was designed for a single-cylinder research engine. There were two main goals to be fulfilled by the new part: allow optical accessibility for applying as many techniques as possible for investigating liquid/gaseous fuel jets and extend the achievable load range in terms of throttling. A secondary objective was to allow multiple injectors to be fitted so as to render dual fueling (e.g., gas/liquid) possible while keeping the existing GDI fuel system.

The design and validation process confirmed through the finite element analysis, both static and dynamic, the reliability of the new component. It successfully passed the maximum stress test, correlated to a boost pressure of 1.5 bar (relative pressure). Safety factor values were over 2.7, and deformation was within acceptable limits.

Another important aspect is that the part is an assembly of volumes with simple geometry and thus can be obtained from standard semi-finished materials. The actual tools and procedure for working each sub-component are also standard and do not require any molding; this is a major advantage in terms of cost when considering the fact that the part is not intended for mass production.

Actually, integration of the part with the engine was ensured by designing the coupling flange so as to guarantee seamless fitting. Finally, the functionality of the new manifold was checked by performing 0D/1D simulations. Compared with the outgoing component, the achievable load range was significantly increased (almost doubling it) while ensuring comparable WOT volumetric efficiency.

As an overall conclusion, it can be stated that the new design completely matches the goals set at the beginning of the development phase and fully fits functionality requirements while enhancing the flexibility of use for the specific application of a research engine.

Author Contributions: Conceptualization, S.S.M. and A.I.; methodology, S.S.M. and A.I.; software, A.I. and G.C.; formal analysis, G.C.; investigation, A.I. and G.C.; resources, A.I.; data curation, G.C.; writing—original draft preparation, A.I.; writing—review and editing, A.I. and G.C.; visualization, S.S.M.; supervision, A.I. and S.S.M.; project administration, S.S.M. and A.I. All authors have read and agreed to the published version of the manuscript.

Funding: This research received no external funding.

Data Availability Statement: Not applicable.

Acknowledgments: The authors acknowledge Carlo Rossi for the technical support.

Conflicts of Interest: The authors declare no conflict of interest.

References

1. Samaras, Z.; Kontses, A.; Dimaratos, A.; Kontses, D.; Balazs, A.; Hausberger, S.; Ntziachristos, L.; Andersson, J.; Ligterink, N.; Aakko-Saksa, P.; et al. *A European Regulatory Perspective towards a Euro 7 Proposal*; SAE Technical Paper: 2022-37-0032; SAE International: Warrendale, PA, USA, 2022. [CrossRef]
2. Heywood, J.B.; Welling, O. Trends in Performance Characteristics of Modern Automobile SI and Diesel Engines. *SAE Int. J. Engines* **2009**, *2*, 1650–166262. [CrossRef]
3. Rakopoulos, C.D.; Hountalas, D.; Zannis, T.; Levendis, Y. *Operational and Environmental Evaluation of Diesel Engines Burning Oxygen-Enriched Intake Air or Oxygen-Enriched Fuels: A Review*; SAE Technical Paper: 2004-01-2924; SAE International: Warrendale, PA, USA, 2004. [CrossRef]
4. Zannis, T.C.; Hountalas, D.T. DI diesel engine performance and emissions from the oxygen enrichment of fuels with various aromatic content. *Energy Fuels* **2004**, *18*, 659–666. [CrossRef]
5. Abidi, S.H.; Hasan, M.M. Review on Studying Effects of Enhancing Turbulence by Modifying the Intake Manifold of Internal Combustion Engine. In *Recent Advances in Mechanical Engineering, Lecture Notes in Mechanical Engineering*; Muzammil, M., Chandra, A., Kankar, P.K., Kumar, H., Eds.; Springer: Singapore, 2021; pp. 361–368. [CrossRef]
6. Singla, S.; Sharma, S.; Gangacharyulu, D. Study of design improvement of intake manifold of internal combustion engine. *Int. J. Eng. Technol. Manag. Appl. Sci.* **2015**, *3*, 234–242.
7. Heywood, J.B. *Internal Combustion Engine Fundamentals*; McGraw Hill: New York, NY, USA, 1988.
8. Delogu, M.; del Pero, F.; Romoli, F.; Pierini, M. Life cycle assessment of a plastic air intake manifold. *Int. J. Life Cycle Assess.* **2015**, *20*, 1429–1443. [CrossRef]

9. Silva, E.A.A.; Ochoa, A.A.V.; Henríquez, J.R. Analysis and runners length optimization of the intake manifold of a 4-cylinder spark ignition engine. *Energy Convers. Manag.* **2019**, *188*, 310–320. [CrossRef]
10. Ceviz, M.A.; Akın, M. Design of a new SI engine intake manifold with variable length plenum. *Energy Convers. Manag.* **2010**, *51*, 2239–2244. [CrossRef]
11. Alves, L.O.F.T.; dos Santos, M.G.D.; Urquiza, A.B.; Guerrero, J.H.; de Lira, J.C.; Abramchuk, V. *Design of a New Intake Manifold of a Single Cylinder Engine with Three Stages*; SAE Technical Paper: 2017-36-0172; SAE International: Warrendale, PA, USA, 2017. [CrossRef]
12. Taylor, J.; Gurney, D.; Freeland, P.; Dingelstadt, R.; Stehlig, J.; Bruggesser, V. *Intake Manifold Length Effects on Turbocharged Gasoline Downsizing Engine Performance and Fuel Economy*; SAE Technical Paper: 2012-01-0714; SAE International: Warrendale, PA, USA, 2012. [CrossRef]
13. Shinde, P.A. Research and optimization of intake restrictor for Formula SAE car engine. *Int. J. Sci. Res. Publ.* **2014**, *4*, 1–5.
14. Castellano, A.; Leone, D.; Cammalleri, M. Design of a Hybrid Electric Power-Split Transmission for Braking Energy Recovery in a Drilling Rig. *Designs* **2022**, *6*, 74. [CrossRef]
15. Diéguez, P.M.; Urroz, J.C.; Sáinz, D.; Machin, J.; Arana, M.; Gandía, L.M. Characterization of combustion anomalies in a hydrogen-fueled 1.4 L commercial spark-ignition engine by means of in-cylinder pressure, block-engine vibration, and acoustic measurements. *Energy Convers. Manag.* **2018**, *172*, 67–80. [CrossRef]
16. Abdellatif, Y.M.; Saker, A.T.; Elbashir, A.M.; Ahmed, S.F. Combustion and Emissions of a Gas-to-Liquid Diesel Engine Utilizing Optimized Spiral-Helical Intake Manifold Designs. *ASME. J. Energy Resour. Technol.* **2021**, *143*, 062308. [CrossRef]
17. Ceviz, M.A. Intake plenum volume and its influence on the engine performance, cyclic variability and emissions. *Energy Convers. Manag.* **2007**, *48*, 961–966. [CrossRef]
18. Elbashir, A.M.; Saker, A.T.; Ahmed, S.F. Effect of Utilizing a Novel Intake Manifold Design on Smoke Emissions and Particulate Size Distributions of a Gas-to-Liquid Diesel Engine. *ASME. J. Energy Resour. Technol.* **2022**, *144*, 022301. [CrossRef]
19. Sadeq, A.M.; Bassiony, M.A.; Elbashir, A.M.; Ahmed, S.F.; Khraisheh, M. Combustion and emissions of a diesel engine utilizing novel intake manifold designs and running on alternative fuels. *Fuel* **2019**, *255*, 115769. [CrossRef]
20. Kadarohman, A.; Khoerunnisa, F.; Sapee, S.; Eko Sardjono, R.; Izzudin, I.; Hendrawan; Mamat, R.; Yusop, A.F.; Erdiwansyah; Yusaf, T. The Effect of Oxygenated Turpentine Oil Additive in Diesel Fuel on the Performance and Emission Characteristics in One-Cylinder DI Engines. *Designs* **2021**, *5*, 73. [CrossRef]
21. Sick, V. Optical diagnostics for direct injection gasoline engine research and development. In *Advanced Direct Injection Combustion Engine Technologies and Development*; Hua Zhao, Ed.; Woodhead Publishing Limited: Sawston, UK, 2009; Chapter 10; pp. 260–286; ISBN 978-1-84569-389-3.
22. Ikeda, Y. The Interaction between In-Cylinder Turbulent Flow and Flame Front Propagation in an Optical SI Engine Measured by High-Speed PIV. *Energies* **2022**, *15*, 2783. [CrossRef]
23. Laichter, J.; Kaiser, S.A. Optical Investigation of the Influence of In-cylinder Flow and Mixture Inhomogeneity on Cyclic Variability in a Direct-Injection Spark Ignition Engine. *Flow Turbul. Combust.* **2023**, *110*, 171–183. [CrossRef]
24. Irimescu, A.; Merola, S.S.; Vaglieco, B.M. Towards better correlation between optical and commercial sparks ignition engines through quasi-dimensional modeling of cycle-to-cycle variability. *Therm. Sci.* **2022**, *26*, 1685–1694. [CrossRef]
25. Merola, S.S.; Irimescu, A.; Marchitto, L.; Tornatore, C.; Valentino, G. Effect of injection timing on combustion and soot formation in a direct injection spark ignition engine fueled with butanol. *Int. J. Engine Res.* **2017**, *18*, 490–504. [CrossRef]
26. Johnen, T.; Haug, M. *Spray Formation Observation and Fuel Film Development Measurements in the Intake of a Spark Ignition Engine*; SAE Technical Paper: 950511; SAE International: Warrendale, PA, USA, 1995. [CrossRef]
27. Bruno, B.; Santavicca, D.; Zello, J. *LIF Characterization of Intake Valve Fuel Films During Cold Start in a PFI Engine*; SAE Technical Paper: 2002-01-2751; SAE International: Warrendale, PA, USA, 2002. [CrossRef]
28. Dhyani, V.; Subramanian, K.A. Fundamental characterization of backfire in a hydrogen fuelled spark ignition engine using CFD and experiments. *Int. J. Hydrog. Energ.* **2019**, *44*, 32254–32270. [CrossRef]
29. Jüngst, N.; Frapolli, N.; Wright, Y.M.; Boulouchos, K.; Kaiser, S.A. Experimental and numerical investigation of evaporating fuel films in combustion. *Appl. Energ. Combust. Sci.* **2021**, *7*, 100033. [CrossRef]
30. Gao, J.; Wang, X.; Song, P.; Tian, G.; Ma, C. Review of the backfire occurrences and control strategies for port hydrogen injection internal combustion engines. *Fuel* **2022**, *307*, 121553. [CrossRef]
31. Bowditch, F. *A New Tool for Combustion Research A Quartz Piston Engine*; SAE Technical Paper: 610002; SAE International: Warrendale, PA, USA, 1961. [CrossRef]
32. Irimescu, A. *Back-Pressure and Fuel Type Effects on Exhaust Gas Oxygen Sensor Readings for a Single Cylinder Spark Ignition Engine Running on Gasoline and Ethanol*; SAE Technical Paper: 2019-24-0046; SAE International: Warrendale, PA, USA, 2019. [CrossRef]
33. Gamma Technologies. *GT-SUITE Flow Theory Manual Version 2019*; Gamma Technologies: Westmont, IL, USA, 2019.
34. BOSCH Catalogue, Equipment for High Performance Vehicles, Electronic Throttle Body. Edition 2020. Available online: www.bosch-motorsport.com (accessed on 15 December 2022).